Electronic Supplementary Information

INTEGRATION OF RAPID DNA HYBRIDIZATION AND CAPILLARY ZONE ELECTROPHORESIS USING BIDIRECTIONAL ISOTACHOPHORESIS

S.S. Bahga[a,‡], C.M. Han [a,‡], and J.G. Santiago[a,*]
[‡]*Equal contribution*
[a]*Department of Mechanical Engineering, Stanford University, CA 94305, USA.*

Contents

S1. Choice of electrolyte chemistry for coupling ITP and CZE using bidirectional ITP

In our bidirectional ITP experiments, we use anionic ITP to preconcentrate, mix and hybridize DNA fragments, and cationic ITP to generate a strong counter-migrating pH gradient across the LE+/TE+ interface. We choose initial conditions such that the anionic ITP zones and the cationic ITP shock approach each other and interact (see Figure1a-c in the main article). When the cationic ITP shock wave washes over the focused DNA zones, TE+ replaces LE+ as the counter-ion for anionic ITP. This change in counter-ion of anionic ITP results in a sudden change in pH of the anionic ITP zones. We choose electrolyte chemistry such that the pH change associated with shock interaction causes effective mobility of LE- to decrease to a value lower than the effective mobility of all focused DNA fragments. Consequently, shock interaction disrupts ITP focusing of DNA fragments and triggers electrophoretic separation.

In the current work, we use sodium bicarbonate as the LE+/LE- mixture (sodium ion is LE+ and bicarbonate ion from carbonic acid is LE-), pyridine as TE+ and Hepes as TE-. Figure S1 shows variation of effective mobility of LE-, TE- and DNA fragments for different pH values. Prior to shock interaction, pH of anionic ITP zones is around 8.1. At this pH, effective mobilities of LE- and TE- ions bracket the mobility of DNA fragments, as shown in Figure S1. Therefore, DNA fragments focus in anionic ITP. After shock interaction, pyridine (TE+, $pK_{a,+1} = 5.2$) replaces sodium (LE+, $pK_{a,+1} = 13.7$) as the counter-ion for anionic ITP. Pyridine is a weaker base than sodium hydroxide and so lowers the pH of anionic ITP zones to a value of ~5.7, which is lower than the $pK_{a,-1}$ of carbonic acid ($pK_{a,-1} = 6.4$, $pK_{a,-2} = 10.3$). Therefore, the effective mobility of LE- becomes significantly smaller than the mobility of DNA fragments (which is fairly constant over pH > 5), as shown in Figure S1. Thus, shock interaction in our bidirectional ITP experiments causes DNA fragments to overtake the LE-/TE- interface and separate as in CE. Alternate choices of electrolyte chemistry for coupling ITP with CE using bidirectional ITP exist, and they are discussed in detail by Bahga *et al.*[1]

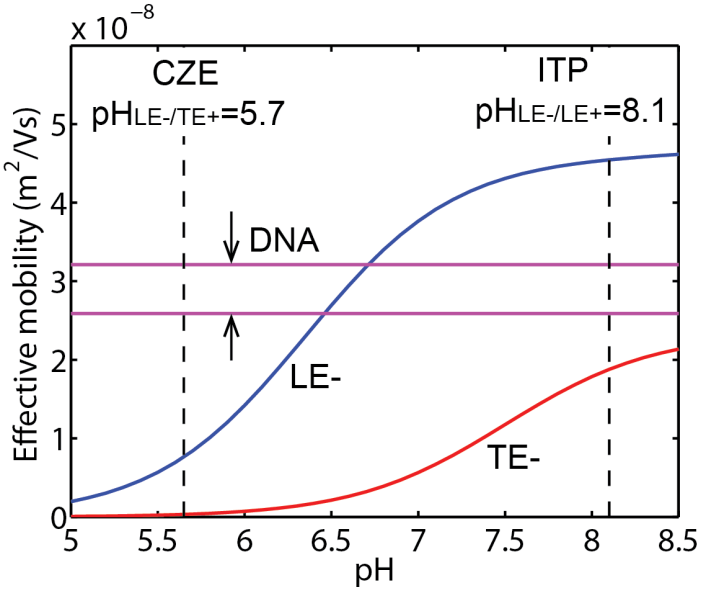

Figure S1: Effective mobilities of LE-, TE- and DNA fragments as a function of pH. LE- is carbonic acid and TE- is Hepes. Prior to shock interaction, the pH of anionic ITP zones is approximately 8.1, and LE- and TE- mobilities bracket the mobilities of DNA fragments. Therefore, DNA fragments focus in ITP. After the interaction of anionic and cationic ITP shocks, the anionic ITP zones are titrated to a pH of 5.7. At the new pH, the mobility of LE- decreases below the mobility of DNA fragments. As a result, DNA fragments overtake LE-/TE- interface and separate as in CZE. We calculated the effective mobilities of LE- and TE- using Peakmaster code[2] by neglecting the effect of

ionic strength. We used a representative range of DNA mobilities, 25.9 – 32.1x10^{-9} $m^2V^{-1}s^{-1}$ for 72-310 nt DNA in 0.6% HEC sieving matrix.[3] According to Costantino *et al.*[4], we assumed pH do not change the effective mobilities of DNA in the pH range from 5 to 8.5.

S2. Experimental setup

We performed all experiments on an inverted epifluorescent microscope (IX70, Olympus, Hauppauge, NY) equipped with a Cy5 filter-cube (Cy5-4040A, Semrock, Rochester, NY). To capture spatiotemporal data (Figures 1d-f) we used a 627 nm LED lamp (LEDC25, ThorLabs, Newton, NJ); a 4× (NA = 0.16) UPlanApo objective (Olympus, Hauppauge, NY); a CCD camera (Micromax1300, Princeton Instruments, Trenton NJ) triggered externally at a frame rate of 4.6 Hz.

For high-sensitivity ITP-CZE experiments (Figure 2) we used a custom point-wise confocal setup coupled to the microscope, similar to that described by Bercovici *et al.*[5] Schematic of the setup is given in Figure S2. We used a 642 nm laser diode (Stradus-642, Vortran Laser Technologies, CA) at 40 mW input power as a light source. The light from laser source was coupled to the microscope though a multimode optical fiber (M31L05) and a beam collimator (F230FC-A), both from Thorlabs, Newton, NJ. The light emitted from fluorescence was collected by the 60× objective and filtered by the emission filter of the Cy5 filter cube. We used a 400 μm pinhole to reject out-of-focus light, and the transmitted light was then refocused on to a photomultiplier tube (PMT) module (H6780-20, Hamamatsu Photonics, Japan). The PMT was powered by a function generator (E3631A, Agilent Technologies, Santa Clara, CA) and operated at a rate of 66.7 Hz (15 ms sampling period with 10 ms integration time). The PMT signal was recorded using the data acquisition unit (C8908, Hamamatsu Photonics, Japan). We applied constant current of 3 μA for the experiments shown in Figures 1d-f, and constant voltage of 1 kV for the experiments shown in Figure 2. In both cases, we used a sourcemeter (model 2410, Keithley Instruments, Cleveland, OH, USA).

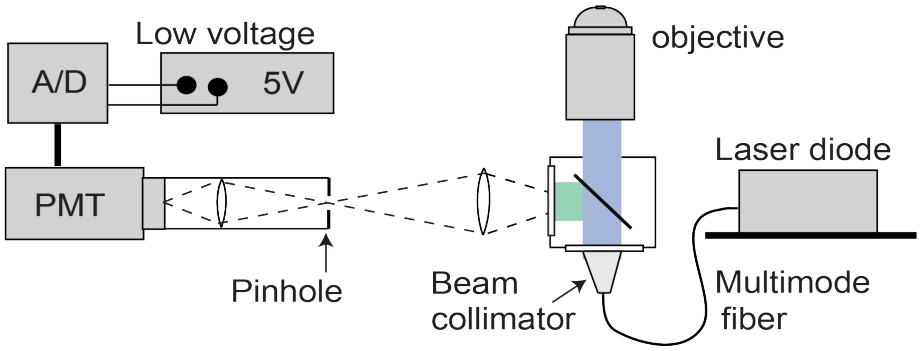

Figure S2: Schematic of our custom pinhole-based, point-confocal microscopy experimental setup. We used a red laser of wavelength 642 nm as a light source. The epifluorescent microscope included a Cy5 filter-cube and a 60×, NA = 0.9 water immersion objective. The 400 μm pinhole in the image plane rejected lights out of the focal plane. For data acquisition, we used photomultiplier tube (PMT) module to record fluorescence intensity as a function of time. See more details in Bercovici *et al.*[5]

S3. Channel geometry and experimental protocol

For all experiments, we used a crown glass microfluidic chip (NS12A, Caliper, Mountain View, CA) consisting of four wet-etched channels arranged in a cross-channel layout. Figure S3 shows a schematic of the microfluidic chip, and the insets provide the channel lengths and the cross-

section dimensions. We measured fluorescence using a point detector located at 44 mm downstream of the West (W) reservoir.

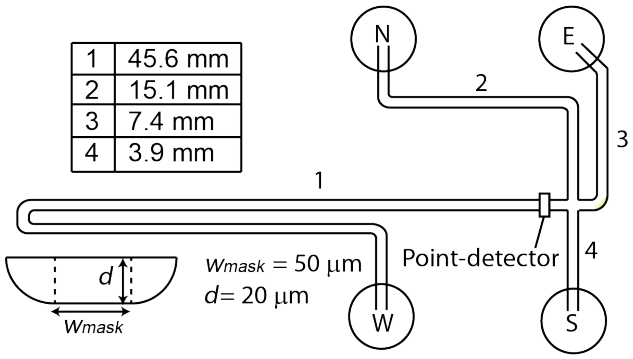

Figure S3: Schematic of Caliper NS12A microfluidic chip and dimensions of microchannels. The inset table provides contour lengths of four channels, and the cross-sectional dimensions are presented in the inset figure. A point detector was located at length 44 mm from the reservoir labeled W.

In Figure S4 we provide further details on the injection protocol for our bidirectional ITP experiments.

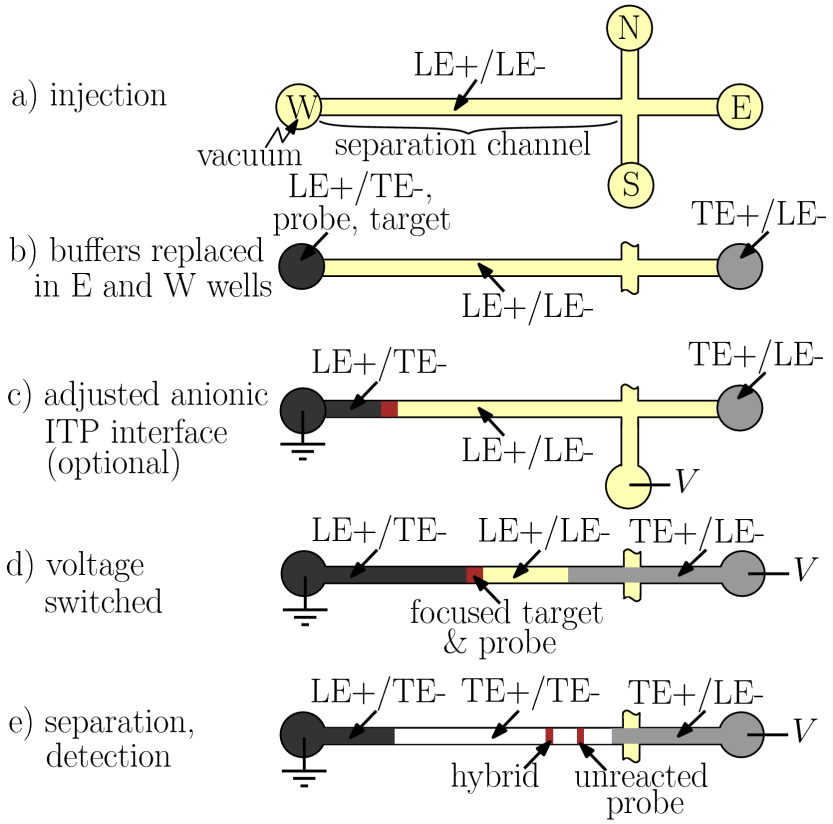

Figure S4: Protocol for performing coupled ITP-based hybridization and CZE separation using bidirectional ITP. For bidirectional ITP experiments on Caliper NS 12A chips: (a) we injected LE+/LE- mixture by filling the N, S, and E wells, then applying vacuum to the W well. (b) We then emptied the E and W wells and filled them with TE+/LE- and LE+/TE- mixtures, respectively. The

DNA target and probe were initially mixed with anionic TE (LE+/TE- mixture). (c) As an optional step, we preconcentrated target and probe DNA fragments in anionic ITP by applying voltage between W and S wells. This step is ensures that target and probe have longer time to hybridize. (d) We then switched voltage across E and W wells. This step initiates bidirectional ITP, and is therefore characterized by anionic and cationic ITP fronts approaching each other. (e) After shock interaction, unreacted probe and target-probe hybrid separate electrophoretically. We imaged the separated DNA fragments close to the cross-junction. We stress that, bidirectional ITP can be set up with simpler protocols without any voltage switching steps (see Figure 1 of the main paper).

S4. Signal analysis of hybridization data from point detector

Here, we describe the signal analysis method used to extract target-probe hybrid peak magnitudes from measured electropherograms. As shown in the inset of Figure 2 of the main paper, the electropherogram of the negative control contains a single peak corresponding to unreacted molecular beacon (MB) probe. When a target DNA fragment is added to the system, a second peak corresponding to target-probe hybrid appears. For the case depicted in Figure 2, peaks corresponding to unreacted 39 nt MB probe and 39 nt target-probe hybrid partially overlap due to very small difference in their mobilities. Therefore, to estimate the actual contribution to signal of the target-probe hybrid, we subtract the signal of negative control from the hybridization signal.

For signal analysis, we first time-shift and scale the unreacted probe peak in negative control signal to register (along time axis) the peak intensity of unreacted probe peak (left black peak in the inset of Figure 2) to the hybridization signal, as shown in Figure 2. This registration makes the analysis robust to slight run-to-run variations in the time of arrival of the peak. We then subtract the scaled unreacted probe peak from the hybridization signal. This subtraction yields a single peak corresponding to the target-probe hybrid. We use the peak magnitude, h, of the resulting target-probe hybrid peak as a measure of amount of hybrid produced during ITP-hybridization. Note that the above approach works only when the shape of unreacted probe peak in hybridization signal is similar to that of negative control. In our experiments the probe concentration is approximately 10-fold larger than the target concentrations. Therefore consumption of small amount of probe during hybridization does not appreciably change the shape of unreacted probe peak.

S5. Modeling of concentration of target-probe hybrid in bidirectional ITP

In Figure 2 of the main paper, we show empirically that the magnitude of target-probe hybrid peak is directly proportional to the initial concentration of target ssDNA mixed in TE, $\left(h \propto c_{T,0}\right)$, if the probe concentration is significantly higher than the target concentration. Here, we justify and analyze this empirical relation with a mathematical model of concentration of target-probe hybrid in bidirectional ITP based ITP-CZE. Our bidirectional ITP experiments involve two distinct steps: (i) ITP preconcentration and hybridization of target and probe DNA fragments, and (ii) CZE separation of reaction products. Since transition from ITP to CZE in bidirectional ITP is nearly instantaneous relative to other time scales, we model ITP and CZE steps individually and couple them at the point where ITP transitions to CZE.

ITP-based hybridization has been studied in detail by Bercovici *et al.*[5] for the case where target and probe species are continuously injected into the system using electrokinetic injection. Assuming pseudo first-order hybridization kinetics, which apply to hybridization reactions with one excess reactant, Bercovici *et al.* derived an analytical expression for the concentration of target-probe hybrid in ITP. Their model is applicable to the current case as the concentration of probe in our experiments is significantly higher than that of target. Following Bercovici *et al.*,[5] and assuming excess probe concentration, the concentration of target-probe hybrid, $c_{TP}\left(x,t\right)$, during ITP-based hybridization is given by,

$$c_{TP}\left(x,t\right)=c_{T,0}f\left(t,\{\mu_i\},k_{on},V_{ITP},\delta_{ITP},c_{P,0},c_{LE},c_{TE}\right)\exp\left(\frac{-\left(x-V_{ITP}t\right)^2}{2\delta_{ITP}^2}\right). \quad (1)$$

Here $c_{T,0}$ and $c_{P,0}$ are the initial concentrations of target and probe, respectively; c_{LE} and c_{TE} are concentrations of LE and TE, respectively; x is the spatial coordinate, t is time, δ_{ITP} is the characteristic thickness of LE/TE interface in ITP and V_{ITP} is the speed of ITP front. In Eq. (1), f determines the production rate of target-probe hybrid, and is a non-linear function of time, on-rate constant $\left(k_{on}\right)$, V_{ITP}, δ_{ITP}, species mobilities, $\{\mu_i\}$, and electrolyte concentrations. Note that only $c_{P,0}$ and not $c_{T,0}$ participates in determining f in this model. Therefore in our experiments, the value of f at the end of ITP preconcentration (at $t=t_{hyb}$) is constant over different runs as we maintain all parameters including the hybridization time and probe concentration constant. We use a constant, $f_{hyb,}$ to denote the value of f at $t=t_{hyb}$. Therefore, at the end of ITP-based hybridization, the concentration of target-probe hybrid is given by,

$$c_{TP}\left(x,t_{hyb}\right)=c_{T,0}f_{hyb}\exp\left(\frac{-\left(x-V_{ITP}t_{hyb}\right)^2}{2\delta_{ITP}^2}\right). \quad (2)$$

The expression for c_{TP} in Eq. (2) serves as the initial concentration for the CZE separation step.

During CZE separation, target-probe hybrid zone migrates and diffuses over time and its concentration can be obtained by solving a linear electromigration-diffusion equation,

$$\frac{\partial c_{TP}}{\partial t}+\mu_{TP}E\frac{\partial c_{TP}}{\partial x}=D_{TP}\frac{\partial^2 c_{TP}}{\partial x^2}. \quad (3)$$

Here, μ_{TP} and D_{TP}, respectively, denote the mobility and diffusivity of the target probe hybrid and E denotes the electric field. Equation (3) along with initial condition at $t=t_{hyb}$ given by Eq. (2) yields the following analytical solution for concentration of target-probe hybrid during CZE step ($t>t_{hyb}$),

$$c_{TP}\left(x,t\right)=c_{T,0}f_{hyb}\frac{\delta_{ITP}}{\left(\delta_{ITP}^2+D_{TP}\left(t-t_{hyb}\right)\right)^{1/2}}\exp\left(-\frac{\left(x-\left(V_{ITP}+\mu_{TP}E\right)t\right)^2}{2\left(\delta_{ITP}^2+D_{TP}\left(t-t_{hyb}\right)\right)}\right). \quad (4)$$

As shown in Eq. (4), the concentration of target-probe hybrid is directly proportional to the reservoir concentration of target, $c_{T,0.}$ In the experiments shown in Figure 2, we varied the initial target concentration without changing other parameters. Therefore, peak magnitudes in Figure 2 vary proportionally with initial target concentration. We note that, the above model is only approximate for our experiment as it assumes constant current operation. In contrast, our experiments shown in Figure 2 were performed by applying constant voltage across the channel. Electrical resistance of the channel varies with time in bidirectional ITP, and so constant voltage operation leads to time varying current density in our experiments. However, this time varying current density does not affect the main conclusion of our model that $c_{TP}(x,t)\propto c_{T,0}$. This is because c_{TP} depends linearly on initial target concentration (see Eqs. (2) and (4)) so this relation also holds all current densities.

S6. Demonstration of multiplexed detection

We performed experiments to demonstrate the feasibility of our assay for multiplexed detection of multiple-length ss-DNA targets. For these experiments we used 39 and 90 nt targets, both having same 27 nt sequence complementary to the MB probe. Figure S5 shows electropherograms for varying concentrations of 39 and 90 nt targets and a fixed concentration of MB probe (1 nM). We observed three well-resolved peaks corresponding to unreacted probe, and target-probe hybrids for 39 and 90 nt targets. For the control experiment where no targets were added to the system, electropherogram shows a single peak corresponding to unreacted probe. We identified the target-probe hybrid peaks by noting the relative change in peak intensities when the concentrations of 39 and 90 nt targets were individually varied in the initial sample (see Figures S5c and S5d).

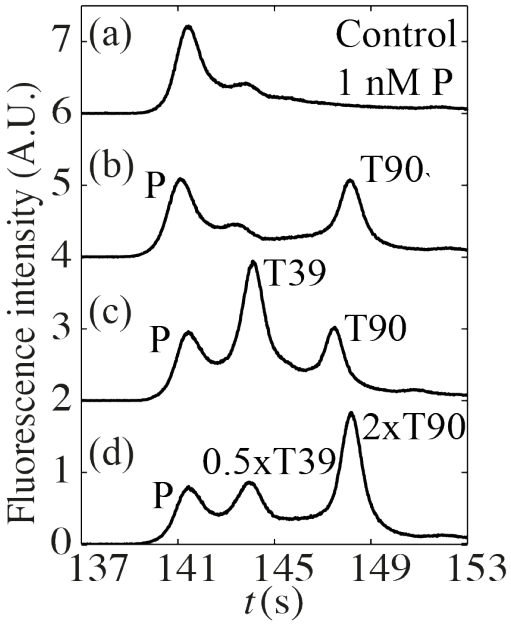

Figure S5: Multiplexed sequence-specific detection of two target oligonucleotides (39 and 90 nt) including the same 27 bases complementary to the molecular beacon probe. Plot shows fluorescent intensity of unreacted probe (P) and target-probe hybrids (T39 and T90) after hybridization and separation. (a) The control case, where no target was present, shows one dominant peak corresponding to the 1 nM probe. (b) When 200 pM of 90 nt target is added with the probe, a second peak corresponding to the hybrid of 90 nt target and probe (T90) appears. The separation between two peaks indicates the effective removal of excess probe from the hybrids. (c) Addition of 39 and 90 nt targets, respectively at 100 and 200 pM, to the probe yields three peaks respectively corresponding to P, T39, and T90. (d) We identified these peaks by noting the relative change in peak intensity upon varying the initial concentrations of 39 and 90 nt targets to 50 and 400 pM, respectively. For these data, we performed anionic ITP focusing for 40 s to enable longer hybridization time and then initiated bidirectional ITP. The abscissa shows the total analysis time, including anionic and bidirectional ITP (during hybridization stage). Electrolyte chemistry and channel geometry are the same as that in Figure 2 of the main text.

S7. ssDNA target sequence information

Here we provide sequences of 39 and 90 nt target ssDNA fragments used in the current study. The 27 bases in the brackets are a part of the 16S rRNA of *E.coli* bacteria,[6] and are complementary to molecular beacon probe. The target and probe DNA were obtained from Integrated DNA

Technologies (IDT, Coralville, Iowa), and 10 μM probe and 100 μM target stock solutions were stored at -20°C.

- 39 nt ssDNA target sequence: TAG ATA [CCC TGG TAG TCC ACG CCG TAA ACG ATG] TCG AC
- 90 nt ssDNA target sequence: GGA CGA AGA CTG ACG CTC AGG TGC GAA AGC GTG GGG AGC AAA CAG GAT TAG ATA [CCC TGG TAG TCC ACG CCG TAA ACG ATG] TCG ACT TGG

References

1. S.S. Bahga, R.D. Chambers, J.G. Santiago, *Anal. Chem.*, 2011, **83**, 6154-6162.
2. M. Jaroš, V. Hruška, M. Štědrý, I. Zusková, B. Gaš, *Electrophoresis*, 2004, **25**, 3080-3085.
3. A. E. Barron, W. M. Sunada, H. W. Blanch, *Biotechnol. Bioeng.*, 1996, **52**, 259-270.
4. L. Costantino, V. Vitagliano, *Biopolymers*, 1966, **4**, 521-528.
5. M. Bercovici, C. M. Han, J. C. Liao, J. G. Santiago, *Proc. Natl. Acad. Sci. U. S. A.*, 2012, **109**, 11127-11132.
6. M. Bercovici, G. V. Kaigala, K. E. Mach, C. M. Han, J. C. Liao, J. G. Santiago, *Anal.Chem.* 2012, **83**, 4110-4117.